

## Calculation of optical excitations in cubic semiconductors. II. Second-harmonic generation

Ming-Zhu Huang and W. Y. Ching

*Department of Physics, University of Missouri-Kansas City, Kansas City, Missouri 64110*

(Received 18 August 1992; revised manuscript received 9 November 1992)

The second-harmonic generations in 15 noncentral symmetric cubic semiconductors are systematically studied by the first-principles full band-structure method. The crystals studied are the III-V compounds AlP, AlAs, AsSb, GaP, GaAs, GaSb, InP, InAs, InSb; and the II-VI compounds ZnS, ZnSe, ZnTe, CdS, CdSe, and CdTe. Calculations are focused on the frequency-dependent complex second-order nonlinear optical susceptibilities  $\chi^{(2)}(\omega)$  up to 10 eV and their zero-frequency limits  $\chi^{(2)}(0)$ . A simple scissor operator is applied to adjust the band gaps from the local-density calculations to the experimental values. Large numbers of  $\mathbf{k}$  points in the sum over Brillouin zone are used which are important in resolving structures in the dispersion curves. Comparison with available experimental data on  $\chi^{(2)}(0)$  and  $\chi^{(2)}(\omega)$  shows general good agreement. It is shown that for a well-converged result, sufficiently high conduction-band (CB) states at least 40 eV from the top of the valence band must be included because of the large CB-CB transition-matrix elements. Correlations between the calculated nonlinear optical parameters and other physical parameters such as band-gap and static dielectric constants are also investigated. It is shown that the validity of the Miller's rule with regard to the ratio between linear and nonlinear susceptibilities is limited to the low-frequency range.

### I. INTRODUCTION

In recent years, nonlinear optics has developed into a field of major study because of rapid advances in laser technology.<sup>1-5</sup> Nonlinear optical techniques have been applied to many diverse disciplines such as atomic, molecular, and solid-state physics, materials sciences, chemical dynamics, surfaces and interface sciences, biophysics, and medicine. The development of new advanced nonlinear optical materials for special applications is of crucial importance in technical areas such as optoelectronics, acoustic-optic conversions, optical signal processing, optical computing, and neuro-network implementation. While there are intense efforts in experimenting, designing, fabricating, and searching for various nonlinear optical materials including semiconductors and semiconductor microstructures, ionic compounds, ferroelectric and liquid crystals, organic molecules, glasses and polymers, there is comparatively a much smaller effort to understand the nonlinear optical process in these materials at the microscopic level. Theoretical understanding of the factors that control the figures of merit is extremely important in improving the existing electro-optic materials and in the search for new ones.<sup>5</sup>

Nonlinear optical process refers to the interaction between electronic states of the material with the incident electromagnetic (EM) field (usually in the form of an intense laser beam), which results in the modified EM fields that are different from the original field in frequency, phase, and amplitude. In crystals with no quasiparticle excitations, this is best described by the polarization  $\mathbb{P}$  of the medium as a power series of the incident field  $E(\omega)$  of frequency  $\omega$ . In components, this is given by<sup>6-10</sup>

$$\begin{aligned} \mathbb{P}_i(\omega) = & \sum_j \chi_{ij}^{(1)}(\omega) E_j(\omega) \\ & + \sum_{jk} \chi_{ijk}^{(2)}(\omega = \omega_1 + \omega_2) E_j(\omega_1) E_k(\omega_2) \\ & + \sum_{jkl} \chi_{ijkl}^{(3)}(\omega = \omega_1 + \omega_2 + \omega_3) \\ & \times E_j(\omega_1) E_k(\omega_2) E_l(\omega_3) + \dots, \end{aligned} \quad (1)$$

where  $\chi^{(n)}(\omega)$  is the  $n$ th-order frequency-dependent complex susceptibility.  $\chi^{(1)}(\omega)$  is linear susceptibility related to the usual dielectric tensor  $\epsilon(\omega) = \epsilon_1(\omega) + i\epsilon_2(\omega)$  through

$$\chi^{(1)}(\omega) = (1/4\pi)[\epsilon(\omega) - 1]. \quad (2)$$

$\chi^{(2)}(\omega)$  and  $\chi^{(3)}(\omega)$  are the second- and third-order nonlinear susceptibility tensors of rank three and four, respectively. (From here on, it is implicitly understood that  $\chi^{(n)}$  are the frequency-dependent tensors of appropriate rank unless specifically stated otherwise.) For a simple process of second-harmonic generation (SHG), we have  $\omega_1 = \omega_2 = \omega'$  and  $\omega = \omega_1 + \omega_2 = 2\omega'$  where  $\omega$  is the frequency of the field generated by the polarization of the medium and  $\omega_1, \omega_2$  are the frequencies of the incident field. Similarly, for the third-harmonic generation (THG), we have  $\omega_1 = \omega_2 = \omega_3 = \omega'$  and  $\omega = \omega_1 + \omega_2 + \omega_3 = 3\omega'$ . Hence, for optical harmonic generations, only a single excitation frequency  $\omega$  for  $\chi^{(n)}(\omega)$  is sufficient to specify the frequency dependence of the susceptibilities. Other more complicated processes involve sum and difference frequency generation or  $d$ - $c$  effect, two-photon absorption, the parametric process, the electro-optic linear Kerr effect in  $\chi^{(2)}(\omega)$ , hyper-Raman scattering, anti-Stokes-Raman

scattering, and the Kerr effect for  $\chi^{(3)}(\omega)$ , etc.<sup>7-10</sup> It is also common to label the second-order nonlinear optical coefficient as  $d_{ijk}^{(2)}$ , which is related to the susceptibility tensor by<sup>8</sup>

$$\chi_{ijk}^{(2)}(\omega) = 2d_{ijk}^{(2)}(\omega). \quad (3)$$

Since the maximum number of independent tensor elements in  $\chi_{ijk}^{(2)}(\omega)$  is 18, it is also customary to write the index  $ijk$  for  $\chi_{ijk}^{(2)}(\omega)$  in the contracted form  $\chi_{im}^{(2)}(\omega)$  with  $i = 1, 2, 3$  and  $m = 1-6$ . We shall use the more conventional form of  $\chi_{ijk}^{(2)}(\omega)$  rather than the contracted form. For systems with bond electrons in which the effects of the free charge carriers are neglected, the nonlinear optical property of a material is mainly determined by the magnitudes of  $\chi^{(2)}(0)$  and  $\chi^{(3)}(0)$ .

Direct theoretical calculation of nonlinear susceptibility tensors in (1) is a very formidable task because it must accurately account for the electronic response of the dielectric medium to the external field. Various theoretical models involving plausible approximations have been devised so as to catch the essential features of the nonlinear optical parameters (NOP) without being deluged with unextractable computational complexities. In spite of many attempts to calculate the NOP for semiconductors in the past 20 years or so, consistent agreement between theory and experiment has not been achieved unless somewhat arbitrary adjustable parameters were introduced either explicitly or implicitly.<sup>11-21</sup> The calculated parameters can sometimes differ from the measured ones by orders of magnitude.<sup>21,22</sup> This predicament can usually be traced to the approximate nature of the calculation, both in the theoretical formulation for the nonlinear optical parameters and in the ways the electronic states were determined. Furthermore, subtle effects such as local-field effect, exciton dynamics, and other types of many-body interactions can also contribute. Of equal importance is that experimental measurements were not always reliable, thus adding to more confusions. Some of the experimental difficulties include the need to account for the vibrational and thermal effects, electrostriction, effects due to finite wave mixing and self-focusing, effects due to sample size, surface quality, and dimension. These factors all add to the uncertainty of the measured data. Very often, the data quoted in the published literature were not from direct measurements, but were extracted by calibrations to measurements on other standard but arbitrarily chosen materials such as  $\alpha$ -quartz,  $\text{KH}_2\text{PO}_4$  (KDP) or  $\text{NH}_4\text{H}_2\text{PO}_4$  (ADP), etc. It is therefore not unusual for the measurements on NOP of the same material to differ by a wide margin.

There are basically two theoretical approaches to studying the nonlinear optical properties in crystals. The first is to use the concept of bond or bond orbitals in which the polarization is expressed as a sum of bond polarizabilities.<sup>11-15,18,20,23</sup> This is an empirical approach that depends on a number of experimental parameters as a meaningful input and does not need accurate wave functions for the electron states. The method is useful for studying general trends among a class of materials with similar bonding characteristics, rather than for a specific crystal. It may break down for systems where the assign-

ment of the bond is not possible.

The other approach is the sum over the actual electronic states of the crystal, or the full band-structure approach. It does require the explicit wave functions of the electronic states. This approach is theoretically more rigorous but computationally much more demanding. Since the requirement for extremely accurate wave functions has rarely been met in the past, the method may not necessarily yield better results than the empirical approach. Aspnes studied  $\chi^{(2)}(0)$  of nine semiconductors with zinc-blende structure using a constant-band-gap model and a constant momentum-matrix-element (MME) approximation.<sup>18</sup> Fong and Shen (FS) (Ref. 21) were the early ones to use a band-structure approach using the empirical pseudopotential method, but obtained a result that was an order of magnitude smaller than the measured data. Recently, a more fundamental full band-structure approach has been advocated by Moss, Sipe, and van Driel (MSV) and used to calculate the frequency-dependent nonlinear susceptibilities in cubic semiconductors.<sup>22</sup> MSV had concluded that the severe underestimation from the result of FS is due to their failure to account for accurate MME, not the local-field effect as claimed by FS. However, MSV used a less accurate empirical tight-binding (ETB) model,<sup>24</sup> and also the minimal-basis *semi-ab-initio* linear-combination-of-atomic-orbitals (LCAO) method<sup>25</sup> as discussed in the preceding paper [hereafter referred to as paper I (Ref. 26)]. The band structures were not self-consistent and the number of conduction-band (CB) states included in the calculation were inadequate. So, in spite of rather extensive calculations of both the second-<sup>22,27</sup> and third-harmonic generations<sup>28</sup> for a number of cubic semiconductors and their interfaces,<sup>29,30</sup> the degree of agreement with the measured data was less than desirable. More recently, Levine and Allan (LA) have used the first-principles pseudopotential method in the local-density approximation (LDA) with local-field corrections<sup>31-33</sup> to study the zero-frequency limits  $\chi^{(2)}(0)$  of AlP, AlAs, GaP, and GaAs and obtained values in good agreement with experiment. However, the approach used by LA appears to be unsuitable for the study of the frequency dependence of the harmonic generations; presumably, the formulation is restricted to longitudinal response only.<sup>31</sup> Ma *et al.* (MCKH) have also calculated nonlinear optical parameters for GaAs using a self-consistent pseudofunction method in the LDA approximation.<sup>34</sup>

As discussed in paper I, the band theory is itself a one-electron approximation and may involve further approximations, depending on the specific method and computational strategy chosen. We consider the band approach to be a more fundamental approach that is capable of providing a deeper understanding of the nonlinear optical properties of the materials, even though the results obtained from using the band approach may not always be better than simpler empirical methods.<sup>35</sup> Because of the recent progress in computational band theory based on density-functional theory and great interest in materials with electro-optic applications, calculation of nonlinear optical properties in semiconductors using the band-

structure approach has gained much impetus. Recent results for GaAs appear to become more consistent provided the underlying electronic structure and the optical transition-matrix elements were rigorously calculated, and a sufficient number of CB states are taken into account.<sup>36</sup>

In this paper, we describe a systematic and detailed calculation of the SHG for 15 non-centro-symmetric compound semiconductors with zinc-blende structure, namely, the III-V compounds AlP, AlAs, AlSb, GaP, GaAs, GaSb, InP, InAs, InSb; and the II-VI compounds ZnS, ZnSe, ZnTe, CdS, CdSe, and CdTe. The nonlinear optical-response calculation follows the full band-structures approach without local-field correction as was formulated by MSV (Ref. 22), but using the self-consistent orthogonalized-linear-combination-of-atomic-orbitals method (OLCAO) as described in paper I. We emphasize the importance of using accurate self-consistent band-structure results. It is much more meaningful to perform calculations on all cubic semiconductors using a single computational method, to compare and contrast the results obtained, and to observe the general trends. In the paper to follow, the results of the calculation for the third-order susceptibilities in 18 semiconductors will be presented.<sup>37</sup> Preliminary result for GaAs using this approach has already been reported.<sup>36</sup>

The plan for this paper is as follows. In Sec. II, we outline the computational method used for calculating the SHG in some detail. The main results of  $\chi^{(2)}(0)$  and  $\chi^{(2)}(\omega)$  are presented in Sec. III. Section IV is devoted to a discussion of these results with emphasis on possible correlations that may exist, and in comparing with the available experimental data. Also discussed is the validity of the Miller's rule<sup>38</sup> based on the calculated results for semiconductors. The last section gives a brief conclusion of the work completed.

## II. METHOD AND APPROACH

The simplest nonlinear optical materials are the cubic semiconductors. For crystals that are centrosymmetric such as Si and Ge, the dipole SHG  $\chi_{ijk}^{(2)}(\omega)=0$  (or for any

tensor of odd rank) due to inversion symmetry. For non-centro-symmetric compounds such as GaAs and ZnS with a cubic group symmetry, only one independent nonzero element [ $\chi_{123}^{(2)}(\omega)$ ] exists out of a total of 18 tensor elements in  $\chi_{ijk}^{(2)}(\omega)$ . For the  $\chi^{(3)}(\omega)$  tensor, it can be shown that only two independent elements  $\chi_{111}^{(3)}(\omega)$  and  $\chi_{1212}^{(3)}(\omega)$  are nonzero.<sup>10</sup>

In this paper, we will discuss only the calculation of the complex dispersion  $\chi_{123}^{(2)}(\omega)$  for the SHG using the band-structure approach. We start with the electronic structure of a crystal calculated using the first-principles self-consistent OLCAO method, and calculate all the relevant momentum-matrix elements at the regularly spaced  $\mathbf{k}$ -point mesh in the irreducible portion of the Brillouin zone (BZ). The imaginary part  $\text{Im}[\chi^{(2)}(\omega)]$  is evaluated first and the real part  $\text{Re}[\chi^{(2)}(\omega)]$  is then obtained from the imaginary part by the Kramers-Kronig (KK) transformation

$$\text{Re}[\chi^{(2)}(\omega)] = -P \int_0^\infty \frac{\omega'}{\omega'^2 - \omega^2} \text{Im}[\chi^{(2)}(\omega')] d\omega'. \quad (4)$$

The use of (4) to obtain the real part of  $\chi^{(2)}(\omega)$  from the imaginary part is guaranteed from the causality condition.<sup>39</sup> The static limit  $\chi^{(2)}(0)$  can be calculated separately and checked against the one obtained from the real part of  $\chi^{(2)}(\omega)$  at  $\omega=0$ . The end result is the absolute dispersion  $|\chi^{(2)}(\omega)|$ , which is the physical observable that can be compared with experimental measurements. In the actual calculation, the simpler  $\chi^{(2)}(0)$  is calculated first as a function of CB cutoff to determine the level of CB-state convergence needed, which will then be used in the much more time-consuming calculation of the dispersion relations.

Analytical expressions suitable for theoretical computation can be derived using the standard perturbation theory within the density-matrix formalism of quantum mechanics.<sup>40-43</sup> Apparently, different forms of analytical expressions exist. According to MSV, the form using the minimum-coupling scheme is the most amenable to the band theoretical approach. The general expression for  $\chi^{(2)}$  for crystals with cubic symmetry takes the form<sup>22</sup>

$$\bar{\chi}^{(2)}(\omega) = \frac{i}{2} \left[ \frac{e}{m\omega} \right]^3 \sum_{vcc'} \int_{\text{BZ}} \frac{d\mathbf{k}}{4\pi^3} \{ P^{vc} P^{cc'} P^{c'v} \} \left[ \frac{1}{(E_{cv} - 2\hbar\omega)(E_{c'v} - \hbar\omega)} + \frac{1}{(E_{c'v} + 2\hbar\omega)(E_{cv} + \hbar\omega)} + \frac{1}{(E_{cv} + \hbar\omega)(E_{c'v} - \hbar\omega)} \right], \quad (5)$$

where  $v$  stands for a valence-band (VB) state and  $c, c'$  two different conduction-band (CB) states,  $E_{cv}(\mathbf{k}) = E_c(\mathbf{k}) - E_v(\mathbf{k})$  is the difference in band energies between two states  $c$  and  $v$ , and  $\mathbf{P}_{cv} = -i\hbar \int \Psi_c(\mathbf{k}, \mathbf{r}) \nabla \Psi_v(\mathbf{k}, \mathbf{r}) d\mathbf{r}$  is the corresponding MME. It should be noted that in many nonlinear optical calculations with molecular systems,<sup>44</sup> the dipole matrix  $e \int \varphi_i^*(r) r \varphi_j(r) dr$  is usually evaluated instead of the MME  $\mathbf{P}$ . The dipole matrix element is ill defined for Bloch states of the crystal.<sup>45</sup> In the band approach for the nonlinear optical properties, accurate MME between Bloch states is a necessary prerequisite.

We follow MSV (Ref. 22) in writing the  $\text{Im}[\chi^{(2)}(\omega)]$  for crystals with cubic symmetry as

$$\text{Im}[\chi_{123}^{(2)}(\omega)] = -\frac{\pi}{2} \left[ \frac{e\hbar}{m} \right]^3 \sum_{vcc'} \int_{\text{BZ}} \frac{d\mathbf{k}}{4\pi^3} \text{Im}[p_x^{vc} p_y^{cc'} p_z^{c'v}] \left[ \frac{(E_{c'v} - 2E_{cv})\delta(E_{c'v} - \hbar\omega)}{E_{c'v}^3(E_{c'v} + E_{cv})(2E_{c'v} - E_{cv})} + \frac{16\delta(E_{cv} - 2\hbar\omega)}{E_{cv}^3(2E_{c'v} - E_{cv})} \right]. \quad (6)$$

This form has the advantage of separating the  $\text{Im}[\chi^{(2)}(\omega)]$  into two terms, the  $\omega$  term and the  $2\omega$  term, each with a  $\delta$  function in the numerator. The presence of the  $\delta$  function facilitates the calculation of the dispersion relation similar to the linear optical calculation in paper I. In Eq. (6), three states are involved. For the virtual electron process that dominates excitation, one is a VB state  $v$  and the other two are the CB states  $c$  and  $c'$ . The three-state MME product therefore involves the CB-CB matrix element  $\mathbf{P}^{cc'}$ . In the virtual-hole process, the VB-VB MME may be involved. However, the virtual-hole contribution is found to be negligible and is therefore omitted from Eq. (6). It is the presence of  $\mathbf{P}^{cc'}$  in the virtual electron process that makes the calculation of SHG very difficult. First, the CB states in semiconductors are generally very extended, which makes the CB-CB MME large. Second, the large CB-CB matrix effect affects  $\text{Im}[\chi^{(2)}(\omega)]$  at any frequency, including  $\omega=0$ , not just the high-frequency region. This is because the MME product is an overall multiplicative factor to terms with  $\delta$  functions. The overall convergence of (6) is determined by the competition between the energy denominator which goes as  $E^3$ , and the increase in the CB-CB MME when higher and higher CB states are included. Eventually, the high power energy denominator will win and the whole expression converges. For this reason, all nonlinear optical calculations in which only a few CB states are taken into account cannot be trusted. We will return to this point in Sec. III A.

The  $\mathbf{k}$ -space integration in (6) is performed numerically over the irreducible wedge of the BZ in conjunction with

the linear-analytic-tetrahedron<sup>46</sup> method similar to the calculation of  $\chi^{(1)}(\omega)$  in paper I. For linear optical calculation, 89  $\mathbf{k}$  points in the  $\frac{1}{48}$  of the BZ is more than adequate for a well-converged result for  $\chi^{(1)}(\omega)$ . This is not the case with the SHG and THG calculations, because the energy denominators in the expressions for  $\chi^{(2)}(\omega)$  and  $\chi^{(3)}(\omega)$  contain singular factors in addition to the strong  $\mathbf{k}$  dependence of the MME. We have tested the calculation by using 89, 505, and 3345  $\mathbf{k}$  points in the  $\frac{1}{48}$  of the zone (corresponding to dividing the  $\Gamma$ -X axis into 8, 16, and 32 equal divisions). We find that the difference between using 505 and 3345  $\mathbf{k}$  points is about 5% on average. However, calculation of  $\text{Im}[\chi^{(2)}(\omega)]$  using 3345 *ab initio*  $\mathbf{k}$  points for a large number of crystals becomes prohibitively expensive; we have to settle for using 505  $\mathbf{k}$  points in the  $\frac{1}{48}$  of the zone in both the  $\chi^{(2)}(\omega)$  and  $\chi^{(3)}(\omega)$  calculations with the understanding that the  $\mathbf{k}$ -space convergence is estimated to be about 5%. In the actual evaluation, the singularity in Eq. (6) is avoided by deleting the contribution from those  $\mathbf{k}$  points where the energy difference in the denominator is less than 0.001 eV. The MME product contribution to each tetrahedron microzone is taken as the average value of the products at the four corner points of the tetrahedron. With a reasonably large number of tetrahedron zones employed in the present calculation, such a scheme combines efficiency with accuracy.

While the zero-frequency limit  $\chi^{(2)}(0)$  can be obtained from  $\text{Re}[\chi^{(2)}(\omega)]$ , it can also be calculated directly from a separate formula:<sup>22</sup>

$$\chi_{123}^{(2)}(0) = -\frac{3}{2} \left[ \frac{e\hbar}{m} \right]^3 \sum_{vcc'}^{c \neq c'} \int_{\text{BZ}} \frac{d\mathbf{k}}{4\pi^3} \text{Im}[p_x^{vc} p_y^{cc'} p_z^{c'v}] \left[ \frac{E_{c'v}^2(2E_{c'v} + E_{cv}) - E_{cv}^2(2E_{cv} + E_{c'v})}{E_{cv}^4 E_{c'v}^4} \right]. \quad (7)$$

This expression is much easier to evaluate than (6) because the denominator is nonsingular and is calculated by direct summation over the BZ with appropriate weighting factors for each  $\mathbf{k}$  point. The two different ways of calculating  $\chi^{(2)}(0)$  serve as a check for the accuracy of the calculation. We find a difference of no more than 5% in  $\chi^{(2)}(0)$  using the two different approaches for the same number of  $\mathbf{k}$  points used. The internal consistency of the calculation removes any doubt about the possible divergence in (6) as  $\omega$  goes to zero which was the subject of controversy some 20 years ago.<sup>18</sup> The minor discrepancy comes mainly from the numerical procedure for the Kramers-Kronig conversion. We have calculated  $\chi^{(2)}(0)$  according to Eq. (7) as a function of CB energy cutoff  $E_{\text{cf}}$  for each crystal to check for the adequacy of the number of CB states included. We will present the results in Sec. III.

As pointed out in paper I, the LDA calculation for semiconductors underestimates the band gap. Since the role of the band gap becomes even more important in nonlinear optical properties, and calculation beyond the LDA theory is generally very complicated even for linear optical properties (see discussion in paper I), we decided to use the simplest form of scissor operator to enlarge the

band gap for each crystal to its reported experimental value, which is listed in Table I. This strategy is partly justified by the fact that quasiparticle calculation<sup>47-49</sup> on several semiconductors shows a rather uniform upward shift in the CB and apparently with no appreciable change in the CB wave functions. Although a more elaborate form of scissor operator has been suggested,<sup>33</sup> we feel the uncertainty involved in other considerations such as CB convergence, accuracy of the MME, and the adequate number of  $\mathbf{k}$  points, etc., may be more important than a slightly more elaborate form of scissor operator. Furthermore, considering that the present work involves the calculation of a large number of semiconductors, the use of the simpler form of the scissor operator is computationally more expedient. Had no scissor operators been applied, as in the case of  $\chi^{(1)}(\omega)$  in paper I, our calculated  $\chi^{(2)}(0)$  values would be 30-50% larger, but still of the same order of magnitude.

We have neglected other many-body effects such as excitonic effect, local-field effect, and finite-temperature effects, etc. as discussed in I. Even in ionic insulators, where the local-field effect is expected to be more important, a study by Lines<sup>23</sup> shows its effect on the  $\chi^{(3)}(0)$  to be quite small with the correction factor close to 1. The

TABLE I. Calculated second-order nonlinear optical properties of cubic semiconductors. Parentheses following the experimental data indicate either the finite frequency, or  $w$ , which implies the data are for the wurtzite structure;  $zzz$ ,  $zxx$ , etc. specifies the tensor element for wurtzite crystal. For data from other calculations, Refs. 21 and 22 use the band approach and are underlined. For data from Ref. 22, the first number was obtained using the *semi-ab-initio* method, followed by the number in parentheses obtained using the ETB method with MME determined separately. References 32 and 34 use the LDA approach and are in bold type. See text for a more detailed explanation.

Crystal	$E_{cf}$ (eV)	Present calc.	$\chi^{(2)}(0)$ ( $10^{-8}$ esu) Experiment	Other calculations	$\Delta(0)$ ( $10^{-6}$ esu)
AlP	40	4.8		50 <sup>a</sup> <u>4.7<sup>b</sup></u> , <u>7.2<sup>c</sup></u>	0.9
AlAs	40	11.0		142 <sup>d</sup> , 64 <sup>a</sup> , <u>7.2<sup>b</sup></u> , 11 <sup>c</sup>	1.8
AlSb	40	24.6	23.4 <sup>c</sup> (at 1.6 $\mu\text{m}$ )	111 <sup>d</sup> , 70 <sup>f</sup> , 85 <sup>a</sup>	1.8
GaP	40	32.2	34.3 <sup>c</sup> (at 1.6 $\mu\text{m}$ ) 28 <sup>i</sup> (at 1.6 $\mu\text{m}$ ) 52 <sup>m</sup> 19.8 <sup>p</sup> 28 <sup>q</sup>	85 <sup>d</sup> , 140 <sup>f</sup> , 75 <sup>g</sup> , 62 <sup>h</sup> 45 <sup>a</sup> , 56 <sup>j</sup> , 24 <sup>k</sup> , 26 <sup>l</sup> 41 <sup>n</sup> , <u>10.4(38)<sup>o</sup></u> , 17 <sup>c</sup>	1.2
GaAs	40	60	91 <sup>c</sup> (at 1.6 $\mu\text{m}$ ) 171 <sup>i</sup> (at 1.6 $\mu\text{m}$ ) 176 <sup>r</sup> 90 <sup>m</sup> 64 <sup>u</sup> 43 <sup>p</sup> 72 <sup>q</sup>	1.22 <sup>d</sup> , 190 <sup>f</sup> , 108 <sup>g</sup> , 100 <sup>h</sup> 98 <sup>a</sup> , 85 <sup>j</sup> , 38 <sup>k</sup> , 46 <sup>l</sup> , 61 <sup>n</sup> <u>4.0<sup>s</sup>, 24.9(96)<sup>o</sup></u> , 41 <sup>c</sup> , 200 <sup>t</sup>	1.0
GaSb	40	152.9	200 <sup>m</sup> , 300 <sup>m</sup>	235 <sup>d</sup> , 160 <sup>f</sup> , 193 <sup>g</sup> , 360 <sup>h</sup> 115 <sup>a</sup> , 155 <sup>j</sup> , 70 <sup>k</sup> , 104 <sup>l</sup> 108 <sup>n</sup> , 82.2(230) <sup>o</sup>	2.6
InP	40	28.4	68.5 <sup>c</sup>	106 <sup>d</sup> , 280 <sup>f</sup> , 68 <sup>a</sup> , 65 <sup>n</sup>	2.1
InAs	40	174	200 <sup>r</sup> 200 <sup>m</sup>	157 <sup>d</sup> , 410 <sup>f</sup> , 171 <sup>g</sup> , 240 <sup>h</sup> 96 <sup>a</sup> , 112 <sup>j</sup> , 64 <sup>k</sup> , 82 <sup>l</sup> 100 <sup>n</sup> , <u>1.0<sup>s</sup>, 155(450)<sup>o</sup></u>	4.2
InSb	40	466	780 <sup>v</sup> 267 <sup>w</sup>	282 <sup>d</sup> , 650 <sup>f</sup> , 286 <sup>g</sup> , 400 <sup>h</sup> 101 <sup>a</sup> , 198 <sup>j</sup> , 110 <sup>k</sup> , 158 <sup>l</sup> 183 <sup>b</sup> , <u>3.0<sup>s</sup>, 360(920)<sup>o</sup></u>	4.2
ZnS	40	4.8	17 <sup>i</sup> (at 1.6 $\mu\text{m}$ ) 14.6 <sup>r</sup> 7.8 <sup>p</sup> ( $w$ )	16 <sup>d</sup> , 43 <sup>g</sup> , 17 <sup>h</sup> , 19 <sup>a</sup> 35 <sup>j</sup> , 10 <sup>k</sup> , 11 ( $w$ ) <sup>l</sup>	0.8
ZnSe	40	3.8	22 <sup>i</sup> (at 1.6 $\mu\text{m}$ ) 37.4 <sup>r</sup>	19 <sup>d</sup> , 63 <sup>g</sup> , 30 <sup>h</sup> , 27 <sup>a</sup> , 53 <sup>j</sup> 15 <sup>k</sup> , 13 <sup>l</sup> , 34 <sup>n</sup> , <u>4.4<sup>b</sup></u>	0.7
ZnTe	40	14.6	73 <sup>i</sup> (at 1.6 $\mu\text{m}$ ) 44 <sup>r</sup>	53 <sup>d</sup> , 112 <sup>g</sup> , 73 <sup>h</sup> , 51 <sup>a</sup> , 90 <sup>j</sup> 29 <sup>k</sup> , 28 <sup>l</sup> , 64 <sup>n</sup> , 7.3 <sup>b</sup>	3.6
CdS	35	7.4	21 <sup>i</sup> ( $zzz$ ) 12.6 <sup>s</sup> ( $zxx$ ) 13.8 <sup>s</sup> ( $xxz$ )	19 <sup>l</sup> ( $w$ )	4.1
CdSe	40	23.7	54 <sup>i</sup> ( $zzz$ ) 26 <sup>r</sup> ( $zzz$ ) 13.6 <sup>r</sup> ( $zxx$ ) 14.8 <sup>r</sup> ( $xxz$ ) 26 <sup>q</sup> ( $zzz$ ) (at 1.6 $\mu\text{m}$ )	20 <sup>l</sup> ( $w$ )	4.9
CdTe	40	27.6	80 <sup>r</sup> 28.2 <sup>m</sup> (at 28 $\mu\text{m}$ ) 28.2 <sup>w</sup>	27 <sup>d</sup> , 134 <sup>g</sup> , 71 <sup>h</sup> , 60 <sup>a</sup> , 132 <sup>j</sup> 33 <sup>k</sup> , 35 <sup>l</sup> , 84 <sup>n</sup> , 24.8 <sup>b</sup>	0.9

<sup>a</sup>Reference 16.<sup>b</sup>Reference 27.<sup>c</sup>Reference 32.<sup>d</sup>Reference 12.<sup>e</sup>Reference 8.<sup>f</sup>Reference 13.<sup>g</sup>Reference 14.<sup>h</sup>Reference 15.<sup>i</sup>Reference 51.<sup>j</sup>Reference 17.<sup>k</sup>Reference 18.<sup>l</sup>Reference 19.<sup>m</sup>Reference 53.<sup>n</sup>Reference 20.<sup>o</sup>Reference 22.<sup>p</sup>Reference 56.<sup>q</sup>Reference 58.<sup>r</sup>Reference 52.<sup>s</sup>Reference 21.<sup>t</sup>Reference 34.<sup>u</sup>Reference 54.<sup>v</sup>Reference 55.<sup>w</sup>Reference 57.

excitonic effect may be important if one focuses on the optical nonlinearity near the semiconductor band edges.<sup>50</sup> We feel that for nonlinear optical properties, it is more important to establish a consistent set of results for a large number of semiconductors using the simpler LDA formalism that can be compared with experimental data without the necessity of relying on empirical calculations.

### III. RESULTS OF CALCULATION

#### A. $\chi^{(2)}(0)$ and test for conduction-band convergence

From Eq. (6), it is clear that  $\chi^{(2)}(\omega)$  depends on the CB-CB MME, which may be quite large because of the extended nature of the CB Bloch functions. This may lead to the divergence of  $\chi^{(2)}(\omega)$  as higher and higher CB states are taken into account. However, the overall convergence depends on its competition with the energy denominator in (6), which goes as  $E^5$  where  $E$  is the energy separation between the VB and the CB states. Ultimately, the high power dependence of  $E$  in the denominator should win and the results of  $\chi^{(2)}(\omega)$  converge. On the other hand, because the OLCAO-LDA band calculation follows a variational principle, the accuracy of the calculated Bloch function at excessively high CB energy for a specific crystal cannot always be guaranteed. It is possible that the MME diverges faster than the counterbalancing effect of the energy denominator due to accumulated errors. It is therefore extremely important to determine a CB energy cutoff  $E_{cf}$  in order to obtain an accurate and converged result for  $\chi^{(2)}(\omega)$ . To this end, we calculate  $\chi^{(2)}(0)$  as a function of increasing  $E_{cf}$  for each crystal using the simpler expression of Eq. (7) before we proceed with the more difficult and time-consuming calculation of the complex dispersion relation  $\chi^{(2)}(\omega)$ . This problem is not encountered in the linear optical calculation because the MME involved are always between the VB and CB states.

In Figs. 1–5, we present the results of  $\chi^{(2)}(0)$  plotted against the  $E_{cf}$  for each series of the 15 compound semiconductors. In studying these results, the density-of-states (DOS) diagrams of Figs. 8–13 of paper I should be consulted. For most crystals,  $\chi^{(2)}(0)$  converges for  $E_{cf}$  less than 35–40 eV. Some crystals show large fluctuations in  $\chi^{(2)}(0)$  before reaching stable values. However, for GaP, GaAs, and, to a lesser extent, AlSb,  $\chi^{(2)}(0)$  appears to increase, and for CdS and CdSe, to decrease after staying relatively flat for a range of frequency. We interpret this as due to the fact that for these crystals, the CB-state wave functions are not sufficiently accurate at  $E > 50$  eV, which results in erroneous CB-CB MME. We therefore set the  $E_{cf}$  for these crystals to the energy where  $\chi^{(2)}(0)$  is relatively stable. The  $E_{cf}$  values adopted for calculation are listed in Table I. In a less rigorous non-first-principles type of calculation, a maximum of four CB's is likely to be included and even these four bands may not represent the lowest-lying CB's because of significant band crossing, as is evident from the band diagrams shown in paper I. It is very likely that the severe underestimation of  $\chi^{(2)}(0)$  by FS using empirical pseudo-potential band structure is due to the insufficient conver-

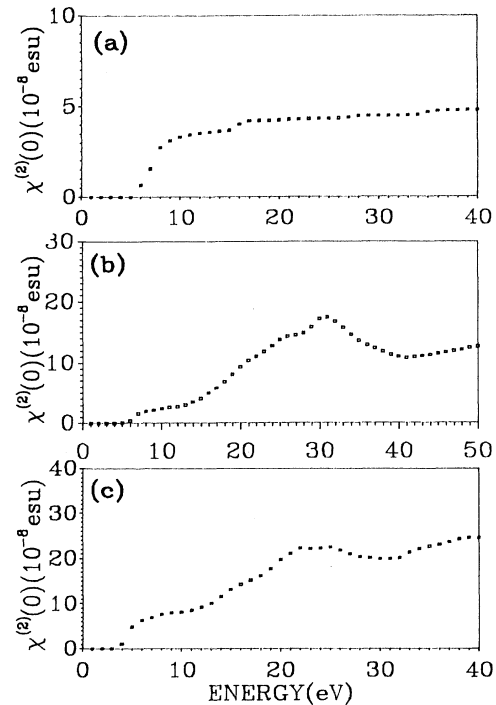


FIG. 1. Calculated  $\chi^{(2)}(0)$  as a function of CB cutoff: (a) AlP, (b) AlAs, and (c) AlSb.

gence in  $E_{cf}$ , and not exclusively due to the inaccuracy of the MME as concluded by MSV. Confusion often arises when other arbitrary parameters (such as the size and magnitude of the MME) were adjusted in order to come up with a reasonable  $\chi^{(2)}(0)$  value without identifying the

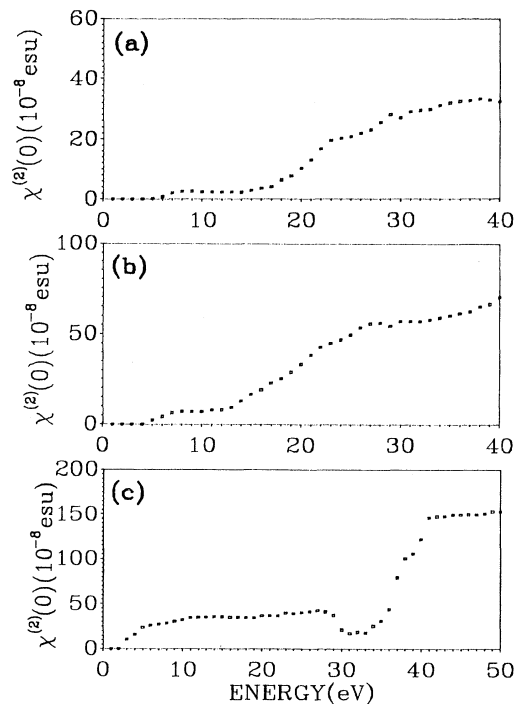


FIG. 2. Calculated  $\chi^{(2)}(0)$  as a function of CB cutoff: (a) GaP, (b) GaAs, and (c) GaSb.

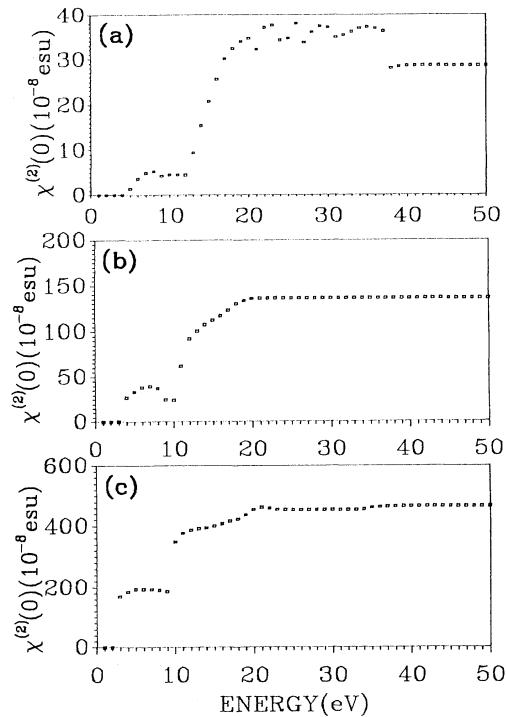


FIG. 3. Calculated  $\chi^{(2)}(0)$  as a function of CB cutoff: (a) InP, (b) InAs, and (c) InSb.

source of the problem. It should be cautioned that the choice of  $E_{cf}$  is not only guided by the convergence consideration and the accuracy of the CB wave functions, but also by the computational practicality of the evaluation of the frequency-dependent dispersion relations. For

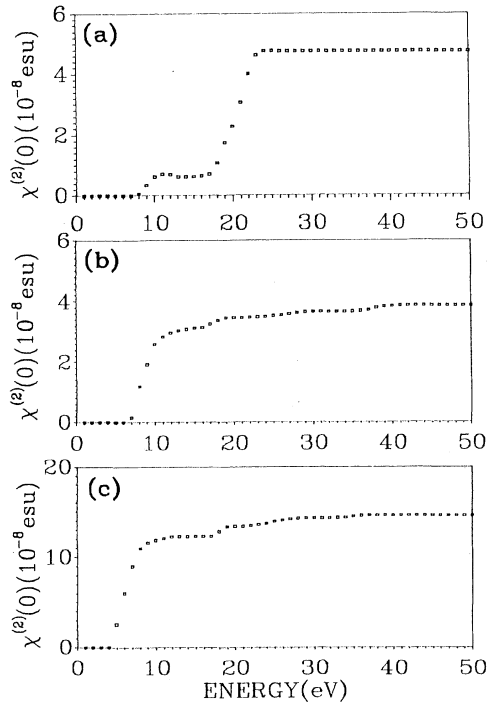


FIG. 4. Calculated  $\chi^{(2)}(0)$  as a function of CB cutoff: (a) ZnS, (b) ZnSe, and (c) ZnTe.

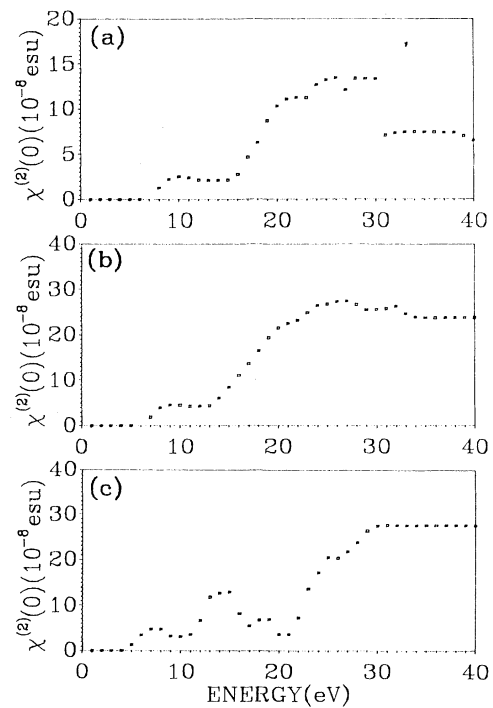


FIG. 5. Calculated  $\chi^{(2)}(0)$  as a function of CB cutoff: (a) CdS, (b) CdSe, and (c) CdTe.

example, in InAs, it is sufficient to use  $E_{cf}=20$  eV while for GaSb, a minimum of 40 eV should be used for  $E_{cf}$ . We are reasonably confident that the cutoff values listed in Table I give sufficient convergence while retaining the accuracy of the CB-CB MME. It should also be noted that the structures in the  $\chi^{(2)}(\omega)$  curves are mainly determined by the energy separation  $E_{ij}$  between the CB and VB states while the amplitudes of the structures depend on  $E_{cf}$ . Our calculated  $\chi^{(2)}(0)$  values, together with the results from other calculations and the measured data<sup>50–58</sup> for the 15 semiconductors, are summarized in Table I.

### B. $\chi^{(2)}(\omega)$ results

The frequency-dependent  $\chi^{(2)}(\omega)$  describes the dynamic nonlinear excitations. Unlike the linear optical properties discussed in paper I, in which the imaginary part of  $\chi^{(1)}(\omega)$  can be directly compared with experimental measurements, the nonlinear dispersion manifests itself as the absolute value of the dispersion that depends on both the real and the imaginary parts. The structures in the  $|\chi^{(2)}(\omega)|$  curve will be quite different from either of  $\text{Re}[\chi^{(2)}(\omega)]$  or  $\text{Im}[\chi^{(2)}(\omega)]$  alone. However, in order to understand the nonlinear optical process at a more microscopic level, it is desirable to investigate the frequency dependency of both  $\text{Re}[\chi^{(2)}(\omega)]$  and the  $\text{Im}[\chi^{(2)}(\omega)]$ . Since the former is obtained from the latter via KK conversion, and the  $\text{Im}[\chi^{(2)}(\omega)]$  consists of two contributions, the  $\omega$  term and the  $2\omega$  term, it is informative to present the results for each contribution as well. In order to be able to make intercomparisons among crystals, we again group the calculated results into each series. In Figs. 6–8, the contributions from the  $\omega$  term and the  $2\omega$

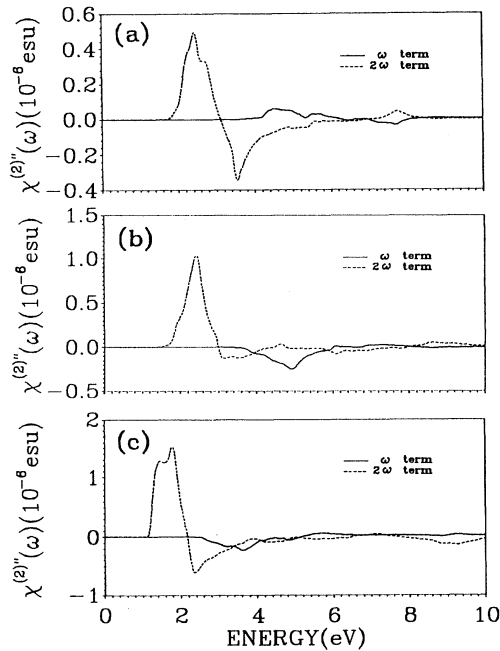


FIG. 6. Contribution to  $\text{IM}[\chi^{(2)}(\omega)]$  from the  $\omega$  term (solid line) and the  $2\omega$  term (dashed line) in (a) AlP, (b) AlAs, and (c) AlSb.

term to  $\text{Im}[\chi^{(2)}(\omega)]$  in the Al, Ga, and In series of the III-V compounds are shown. Similar results for the Zn and Cd series are shown in Figs. 9 and 10, respectively. Our general observations of these dispersion relations are (1) both the  $\omega$ - and  $2\omega$ -term contributions can be positive or negative; (2) the  $2\omega$  term usually dominates in the

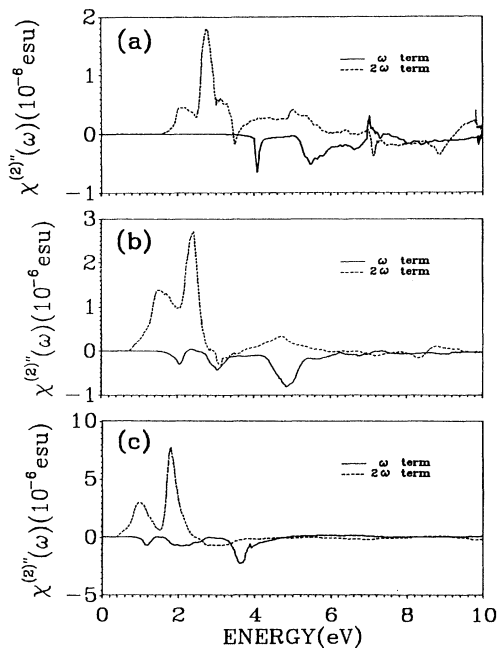


FIG. 7. Contribution to  $\text{IM}[\chi^{(2)}(\omega)]$  from the  $\omega$  term (solid line) and the  $2\omega$  term (dashed line) in (a) GaP, (b) GaAs, and (c) GaSb.

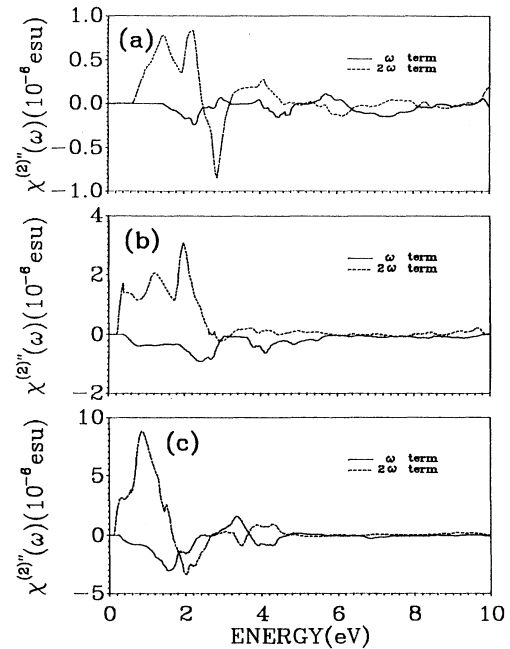


FIG. 8. Contribution to  $\text{IM}[\chi^{(2)}(\omega)]$  from the  $\omega$  term (solid line) and the  $2\omega$  term (dashed line) in (a) InP, (b) InAs, and (c) InSb.

low-frequency region and is positive. It is this feature that ultimately determines the sign and magnitude of  $\chi^{(2)}(0)$  discussed in Sec. III A above. The leading peak in the final  $|\chi^{(2)}(\omega)|$  spectrum originates from the  $2\omega$  resonance term; (3) the  $\omega$  term is also important in determining the overall structure in  $\text{Im}[\chi^{(2)}(\omega)]$ . It is not negli-

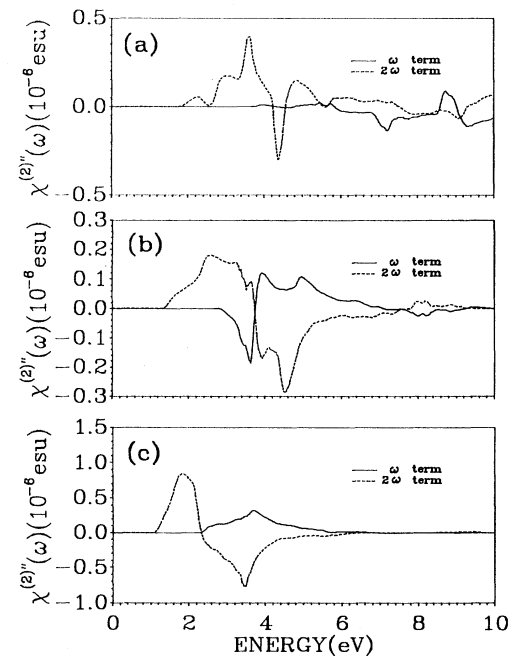


FIG. 9. Contribution to  $\text{IM}[\chi^{(2)}(\omega)]$  from the  $\omega$  term (solid line) and the  $2\omega$  term (dashed line) in (a) ZnS, (b) ZnSe, and (c) ZnTe.

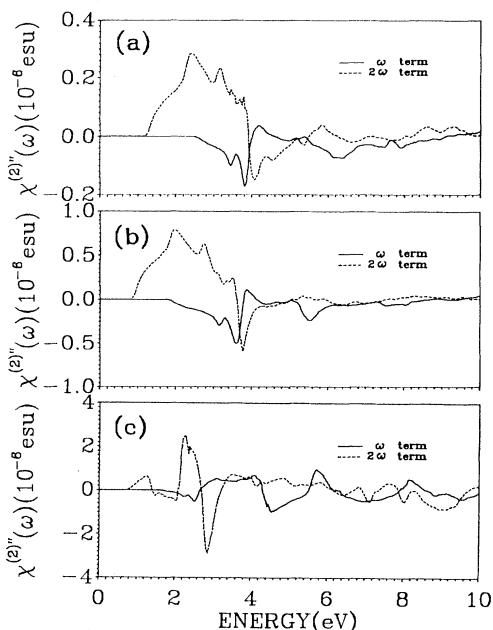


FIG. 10. Contribution to  $\text{Im}[\chi^{(2)}(\omega)]$  from the  $\omega$  term (solid line) and the  $2\omega$  term (dashed line) in (a) HAS, (b) CdSe, and (c) CdTe.

ble; (4) the threshold energies in the  $2\omega$  term are roughly half of the direct gaps at  $\Gamma$ , as are generally expected for the SHG process; (5) in the low-frequency region, the structure in the  $2\omega$  term will ultimately determine the structures in the  $\text{Re}[\chi^{(2)}(\omega)]$  and in  $|\chi^{(2)}(\omega)|$ . This is particularly important for crystals with small band gaps

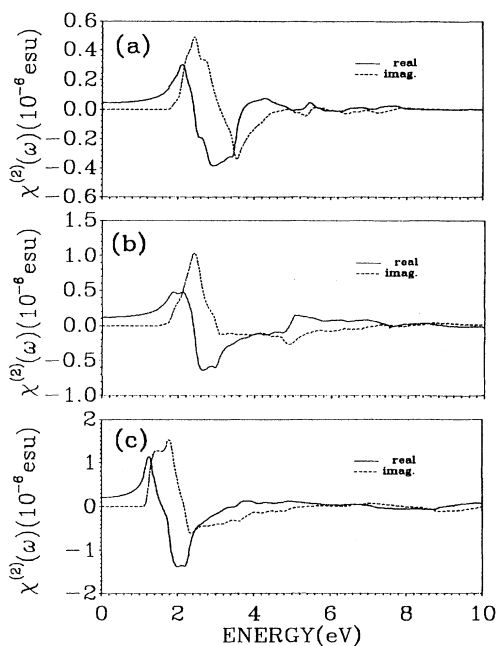


FIG. 11. Calculated real (solid line) and imaginary (dashed line) parts of  $\chi^{(2)}(\omega)$  in (a) AIP, (b) AIAs, and (c) AIsb.

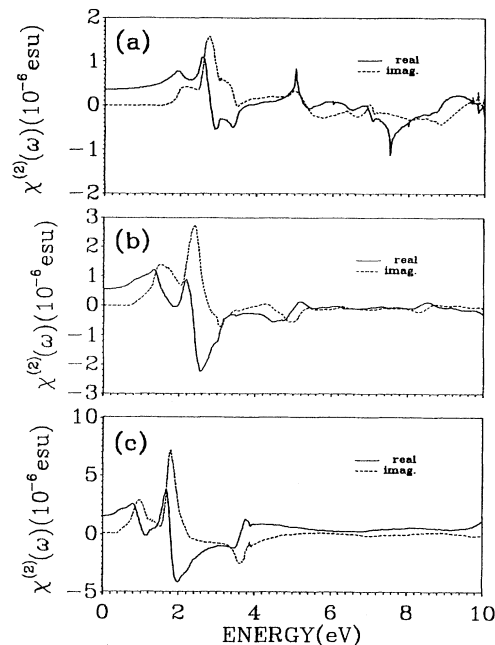


FIG. 12. Calculated real (solid line) and imaginary (dashed line) parts of  $\chi^{(2)}(\omega)$  in (a) GaP, (b) GaAs, and (c) GaSb.

such as InAs and InSb; (6) in the high-frequency region above 5 eV, the  $\omega$ - and the  $2\omega$ -term contribution tend to cancel each other.

The  $\text{Re}[\chi^{(2)}(\omega)]$  and  $\text{Im}[\chi^{(2)}(\omega)]$  for the 15 semiconductors in the five series are shown in Figs. 11–15, respectively. For most crystals, prominent structures are

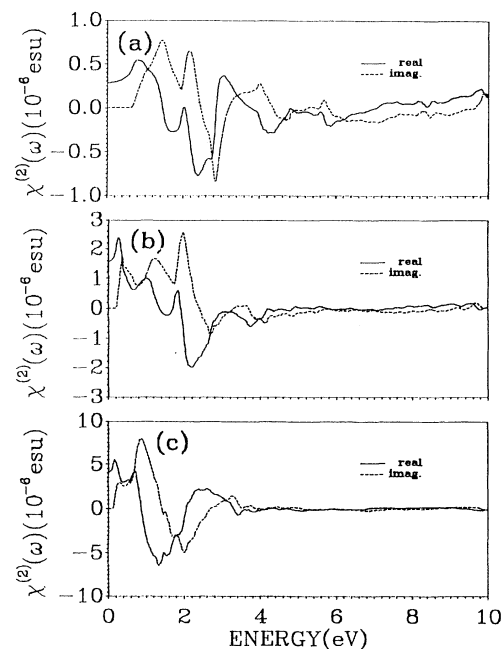


FIG. 13. Calculated real (solid line) and imaginary (dashed line) parts of  $\chi^{(2)}(\omega)$  in (a) InP, (b) InAs, and (c) InSb.

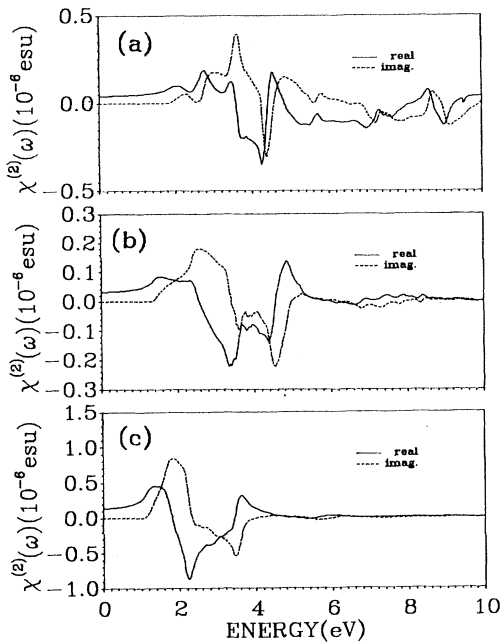


FIG. 14. Calculated real (solid line) and imaginary (dashed line) parts of  $\chi^{(2)}(\omega)$  in (a) ZnS, (b) ZnSe, and (c) ZnTe.

generally limited to the frequency region below 6 eV because of the cancellation of the  $\omega$  and the  $2\omega$  terms in  $\text{Im}[\chi^{(2)}(\omega)]$ . There are exceptions. For example, in GaP, ZnS, and CdTe, substantial structures in both  $\text{Re}[\chi^{(2)}(\omega)]$  and  $\text{Im}[\chi^{(2)}(\omega)]$  up to 10 eV are present. We are unable to provide an explanation for such exceptions other than that they must be related to their fundamental electronic structures. Structures in  $\chi^{(2)}(\omega)$  above 6 eV

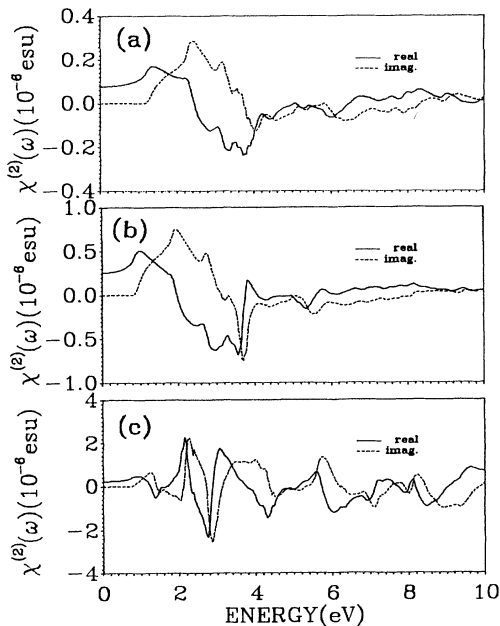


FIG. 15. Calculated real (solid line) and imaginary (dashed line) parts of  $\chi^{(2)}(\omega)$  in (a) CdS, (b) CdSe, and (c) CdTe.

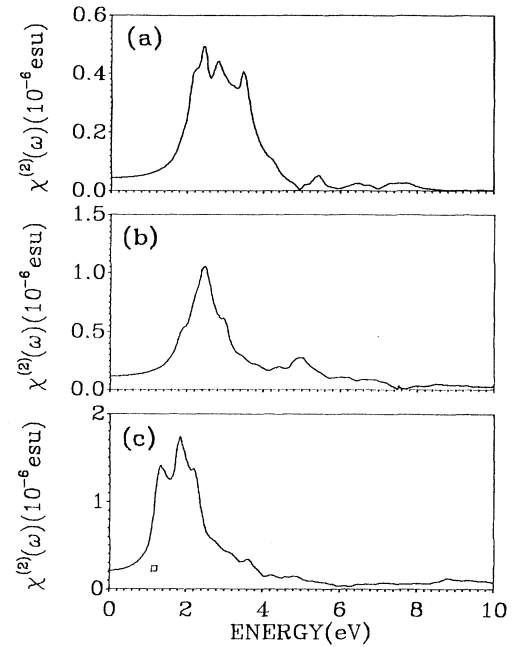


FIG. 16.  $|\chi^{(2)}(\omega)|$  for (a) AIP, (b) AIAs, and (c) AISb. Experimental data, Ref. 5.

are generally less reliable because the higher CB wave functions may be less accurate, as discussed in Sec. III A.

The  $|\chi^{(2)}(\omega)|$  calculated from the  $\text{Re}[\chi^{(2)}(\omega)]$  and  $\text{Im}[\chi^{(2)}(\omega)]$  for the 15 crystals are displayed in Figs. 16–20. It is the dispersion curve  $|\chi^{(2)}(\omega)|$  that will be ultimately compared with whatever measurements are

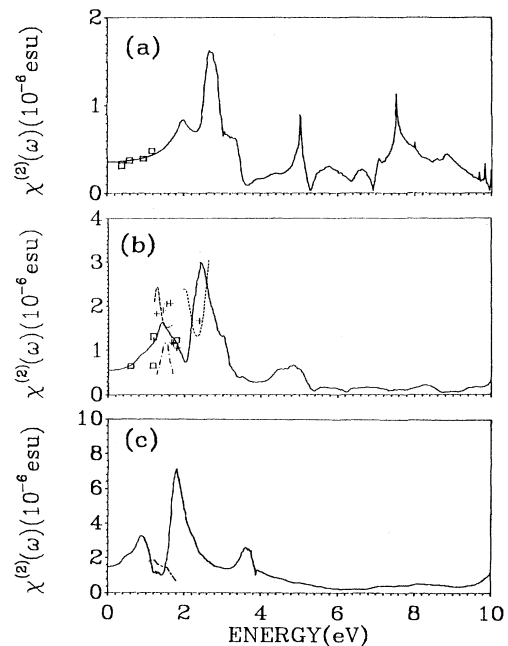


FIG. 17.  $|\chi^{(2)}(\omega)|$  for (a) GaP, experimental data from Ref. 58; (b) GaAs, experimental data: — — — from Ref. 64, . . . . from Ref. 61,  $\square$  from Ref. 8, + from Ref. 63; (c) GaSb, experimental data from Ref. 62.

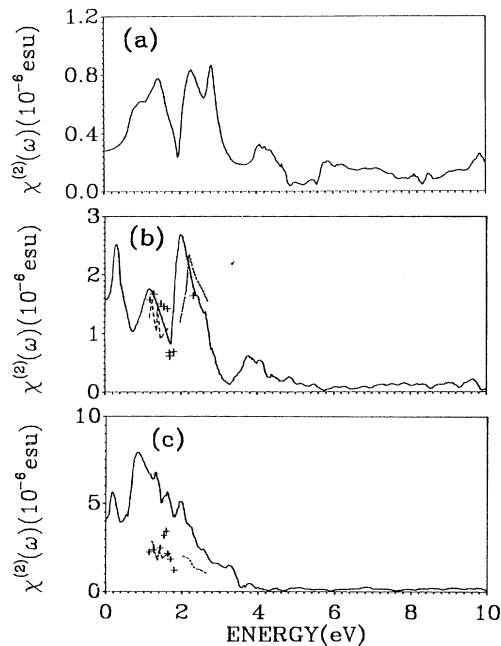


FIG. 18.  $|\chi^{(2)}(\omega)|$  for (a) InP, (b) InAs. Experimental data: — — — from Ref. 60, . . . . from Ref. 61, + from Ref. 63; (c) InSb. Experimental data: — — — from Ref. 60, . . . . from Ref. 61, + from Ref. 63.

available. For GaP, GaAs, GaSb, InAs, InSb, and ZnTe, available experimental data for  $|\chi^{(2)}(\omega)|$  are also plotted. For the Al series, where experimental data are nonexistent, the structures in  $|\chi^{(2)}(\omega)|$  are surprisingly simple and limited to the energy range below 6 eV. For the Ga

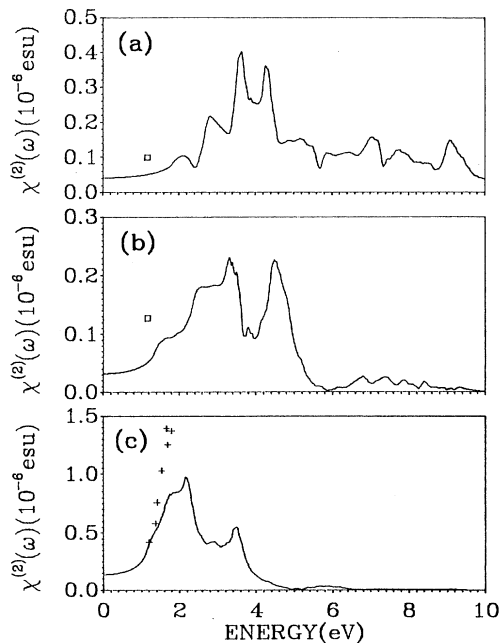


FIG. 19.  $|\chi^{(2)}(\omega)|$  for (a) ZnS. Experimental data from Ref. 8; (b) ZnSe. Experimental data from Ref. 8; (c) ZnTe. Experimental data from Ref. 63.

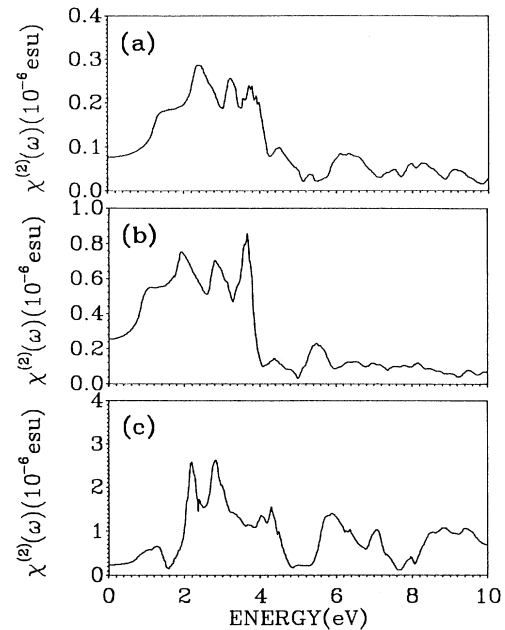


FIG. 20.  $|\chi^{(2)}(\omega)|$  for (a) CdS, (b) CdSe, and (c) CdTe.

series, the low-energy structures below 4 eV consist of a double peak. For the In series, the structures are much more complicated and consist of multiple peaks. For the II-VI compounds, the main difference between the Zn series and the Cd series seems to be that the former consists of double peaks and the latter triple peaks. We also note that within each series, the main peak moves towards lower frequency as the  $Z$  number of the second element increases. These results are further discussed in the next section in comparison with experiment and some other current calculations.

#### IV. DISCUSSION

In Table I, we have listed the calculated<sup>12–22,27,32,34</sup> and measured<sup>50–58</sup> values for  $\chi^{(2)}(0)$  for comparison. The experimental data listed are roughly in chronological order and there are large variations among them. The more recent data are believed to be somewhat more reliable. Some of the data were taken at finite frequencies and are indicated as such. Among the 15 semiconductors studied, we find no experimental data for AlP and AlAs, and the data for CdS and CdSe were for the wurtzite structures. We find excellent agreement with our calculation in six crystals (AlSb, GaP, GaAs, InAs, CdSe, and CdTe), and good agreements with similar orders of magnitude in GaSb, InP, InSb, ZnS, ZnTe, and CdS. Only in one crystal, ZnSe, does the calculated  $\chi^{(2)}(0)$  appear to be an order of magnitude smaller than the available data. We note that for crystals where the agreements are marginal, the data are relatively old and may not be reliable. Given the fact that the experimental data are rather old and scattered, the order-of-magnitude agreement between the calculated and measured  $\chi^{(2)}(0)$  values is what one can realistically hope for. We are unable to locate the

more recent data for  $\chi^{(2)}(0)$  or  $|\chi^{(2)}(\omega)|$  for the cubic semiconductors. In Fig. 21, we plot the calculated  $\chi^{(2)}(0)$  vs the measured values that are judged to be more reliable. The overall agreement is quite satisfactory.

For  $\chi^{(2)}(\omega)$  at finite frequency, the data are much more scarce. For GaAs, InAs, InSb, GaSb, and ZnTe, some limited data are available.<sup>59–64</sup> For AlSb, GaP, ZnS, and ZnTe, single data points at finite frequencies exist. We have plotted these experimental data on the  $|\chi^{(2)}(\omega)|$  curves. It can be seen that the agreement is surprisingly impressive. For GaP, the four data points fall right on the calculated curve. For GaAs, the peaks at 1.4 and 2.4 eV with a deep valley at 2.0 eV are well reproduced by the combination of the data set, although it appears that the peak at 2.4 eV is slightly below the measured data of Bethune, Schmidt, and Shen.<sup>61</sup> Likewise, in InAs, the peaks at 1.2 and 2.0 eV with a deep valley between are well reproduced by three sets of experimental data.<sup>60,61,63</sup> For ZnTe, the data of Chang, Ducuing, and Bloembergen<sup>63</sup> below 2 eV are consistent with the calculated result. In InSb, the measured data appear to be below the calculated ones, but the general profile of the spectrum seems to be in good agreement.

Also listed in Table I are the calculated values for  $\chi^{(2)}(0)$  from other groups. We have compiled the theoretical values for  $\chi^{(2)}(0)$  since 1969. Although several calculated values on the list are in apparent good agreement with experiment, the empirical nature of these calculations makes it less meaningful. We will compare our results with the more recent calculations using the full-band approach. MSV have studied the nonlinear optical susceptibilities of GaP, GaAs, GaSb, InAs, and InSb for photon frequencies up to 4 eV.<sup>22</sup> Ghahramani, Moss, and Sipe later extended the calculation to include ZnSe, ZnTe, and CdTe. Although MSV used a more rigorous full-band-structure approach and provided detailed dispersion curves, their results based on the *semi-ab-initio* band structure were too small and were not in good agreement with the measured data. As pointed out earlier, this could be due to the insufficient number of CB states included in the calculation. By using an ETB model with separately fitted MME, they have improved the

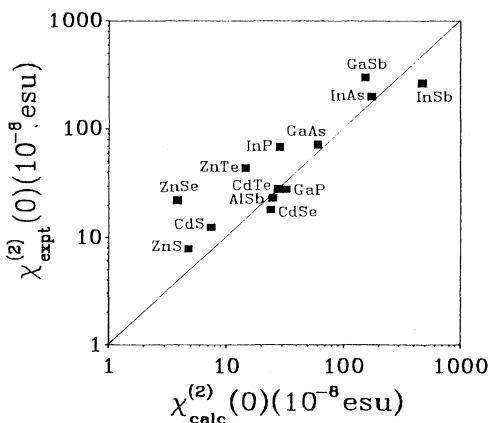


FIG. 21. Calculated  $\chi^{(2)}(0)$  vs experimental  $\chi^{(2)}(0)$ .

agreement with experiment. However, this later approach is rather arbitrary in nature and the quality of such a calculation is difficult to assess. In general, our first-principles results are in much better agreement with the measured data for both  $\chi^{(2)}(0)$  and  $\chi^{(2)}(\omega)$ , especially with the GaP, GaAs, InAs, and InSb crystals.

LA used the first-principles pseudopotential method in the LDA to calculate the  $\chi^{(2)}(0)$  for four semiconductors, AlP, AlAs, GaP, and GaAs. They have also obtained good agreement with experiment and also with our results. They have argued that inclusion of local-field effects and the renormalization of the velocity operator is important. The former can change  $\chi^{(2)}(0)$  by 8–13%. The latter can change the value up to a factor of 2. We have performed test calculations in the GaAs case in which the scissor operator is applied in conjunction with the velocity operator renormalization. We found that the change in  $\chi^{(2)}(0)$  is quite marginal, no more than 12%. We can attribute this difference to the two different methods of electronic-structure calculations as well as the different ways the  $\chi^{(2)}(0)$  are evaluated over the BZ. Most likely, the electronic-structure results calculated by the LDA-OLCAO method have larger gaps and are therefore closer to the experimental values than the work of LA. This, in turn, makes the correction less important. It is difficult for us to estimate how severely this difference will affect the final result. Given the large experimental uncertainty in the nonlinear optical parameters at this time and the complexity of the calculation involved, this question is best left for future studies.

MCKH had calculated the  $\chi^{(2)}(0)$  for GaAs (Ref. 34) using the pseudofunction method of band structure. Their result is a factor of 3–5 greater than ours and that of LA. Since details of their calculation and the information on the electronic structure were not provided, the source of this discrepancy cannot be speculated on. They have also concluded that the correction to the local-field effect should be no more than 3%.

With the 15 compound semiconductors studied, it is feasible to explore any correlations between the NOP and other physical parameters of interest. In Fig. 22, we plot the calculated values of  $\chi^{(2)}(0)$  (in logarithmic scale) vs the direct band gap  $E_g$  at  $\Gamma$ . In spite of a rather large scattering of the data, an approximate linear relationship in Fig. 22 can be established. The general trend is that the smaller-gap semiconductors have larger  $\chi^{(2)}(0)$ . This fact, of course, had been recognized in the early 1960s and was the basis of many empirical calculations of  $\chi^{(2)}(0)$ . In Fig. 23, we plot  $\chi^{(2)}(0)$  (in logarithmic scale) vs the calculated dielectric constant  $\epsilon(0)$  from Table I of paper I. Again, we can identify an approximate linear relationship in Fig. 23 that correlates the larger  $\epsilon(0)$  with larger  $\chi^{(2)}(0)$ . This correlation is not independent of that of Fig. 22 since there is an intimate relationship between the band gap and the dielectric constant  $\epsilon(0)$  of a material. We have to caution the reader that the correlated studies in Figs. 22 and 23 are intended for general trends only, since both the calculated and measured values of  $\chi^{(2)}(0)$  are not of absolute accuracy at this time. What emerges from Figs. 21–23 is the indisputable fact that the calculated and measured values of  $\chi^{(2)}(0)$  for the 15 semi-

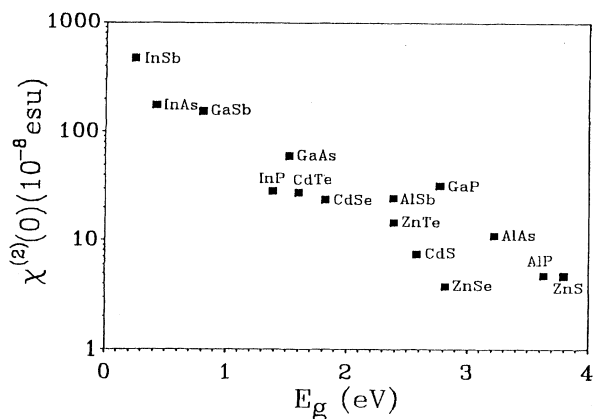


FIG. 22. Calculated  $\chi^{(2)}(0)$  vs measured direct band gap.

conductors are in good agreement and consistent with the general trend.

In 1964, Miller suggested that the second-order susceptibility  $\chi^{(2)}(\omega)$  of a crystal can be related to the linear susceptibility  $\chi^{(1)}(\omega)$  through the following relation based on the analysis of data on a large number of nonlinear optical materials:<sup>38</sup>

$$\chi_{ijk}^{(2)}(2\omega) = \Delta(2\omega)\chi_{ii}^{(1)}(2\omega)\chi_{jj}^{(1)}(\omega)\chi_{kk}^{(1)}(\omega), \quad (8)$$

where  $\Delta(\omega)$  is supposed to be a slowly varying function of  $\omega$  and  $\Delta(0)$  a universal constant. Combining the results of  $\chi^{(1)}(\omega)$  of paper I and  $\chi^{(2)}(\omega)$  of this paper, we are in a unique position to check Miller's rule based on the first-principles results. The results for  $\Delta(\omega)$  are shown in Fig. 24 for the following five representative crystals from each group: (a) AlAs, (b) GaAs, (c) InP, (d) ZnS, (e) CdS. The  $\Delta(\omega)$ 's for other crystals exhibit a similar trend and are not shown. It can be seen that in the low-frequency range below the threshold of  $\text{Im}[\chi^{(2)}(\omega)]$ ,  $\Delta(\omega)$  is approximately constant. Within half an eV of this threshold,  $\Delta(\omega)$  can be considered a slowly varying function of  $\omega$ , and beyond that region,  $\Delta(\omega)$  varies rather rapidly. Therefore, Miller's rule may not be adequate to predict

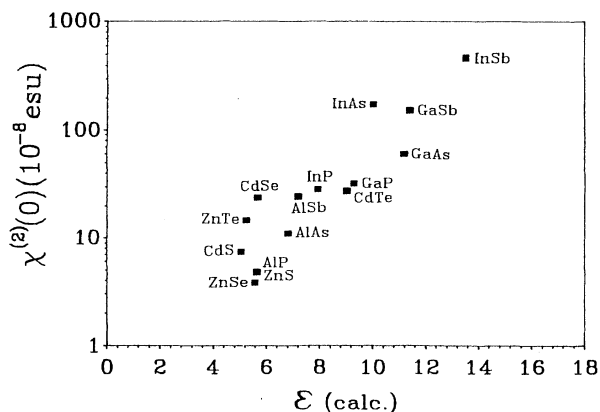


FIG. 23. Calculated  $\chi^{(2)}(0)$  vs calculated  $\epsilon(0)$ .

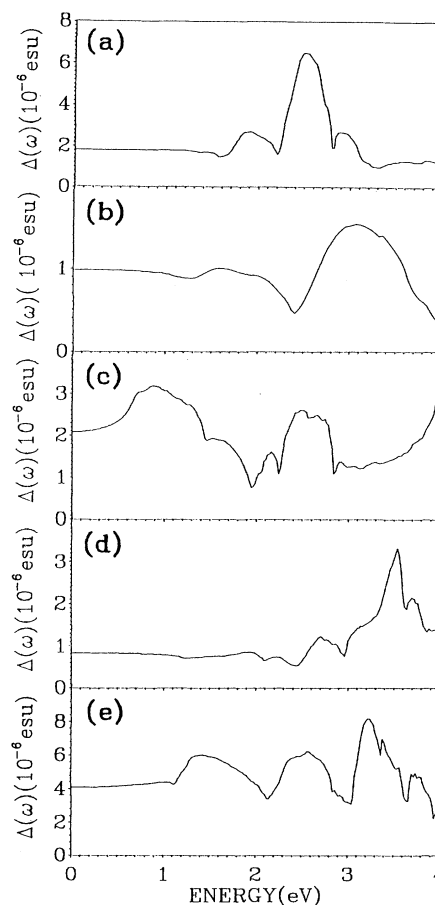


FIG. 24. Check on the Miller's rule for (a) AlAs, (b) GaAs, (c) InP, (d) ZnS, (e) CdS.

$\chi^{(2)}(\omega)$  of a material at finite frequencies above the absorption threshold based on the linear optical properties alone. The  $\Delta(0)$  for the 15 semiconductors are listed in Table I and also plotted in Fig. 25. They vary between 1 and 5 and therefore can hardly be considered a universal constant. But as pointed out by Miller,<sup>38</sup> the  $\chi^{(2)}(0)$  for many nonlinear optical materials can vary over several orders of magnitude; the  $\Delta(0)$  result for the 15 semiconductors shown in Fig. 25 at least lend partial support for

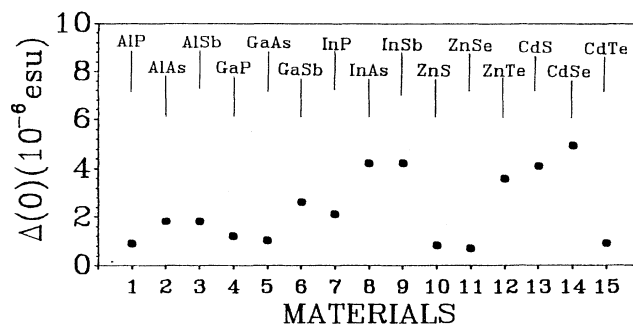


FIG. 25. Calculated Miller's constant  $\Delta(0)$  for the 15 semiconductors.

Miller's conviction. Finally, we need to point out that the above estimation is not very precise because the  $\chi^{(2)}(\omega)$  calculation here is gap corrected while the  $\chi^{(1)}(\omega)$  calculation of paper I has no gap correction and this could cause some errors in  $\Delta$ . However, because of the general correlations between  $E_g$ ,  $\chi^{(1)}(0)$ , and  $\chi^{(2)}(0)$  as discussed above, we believe our assessment of the validity of Miller's rule is still qualitatively valid.

## V. CONCLUSION

We have used the first-principles OLCAO method of band-structure calculation to study the second-order nonlinear susceptibility, or the SHG in 15 cubic compound semiconductors. Results are presented for both the frequency-dependent  $\chi^{(2)}(\omega)$  and its static limit  $\chi^{(2)}(0)$ . Good agreement with experimental values has been obtained on almost all the crystals in spite of the variations over two orders of magnitude. Our calculation has revealed the importance of taking sufficient numbers of CB states in the sum-over-states, full-band-structure calculation for nonlinear excitations because of the large CB-CB MME's. The calculated results are correlated with other physical constants such as the direct band gap and the dielectric constants. The much-celebrated Miller's rule introduced more than 20 years ago is checked and found to be only partially valid.

While the present work demonstrates that the first-principles band-structure method is a very viable approach to studying the nonlinear optical properties of

materials, and that the self-consistent OLCAO method, in conjunction with a "naive" gap-correction procedure, is very effective for such complex calculations, there are still several areas for future improvement. This includes the proper extension beyond the LDA theory and to accurately account for other many-body effects that may become important in nonlinear excitations, especially those that involve highly excited states. Nevertheless, the present result and that of the calculations on the third-order nonlinear susceptibilities in the paper to follow give us great confidence that the nonlinear optical properties of some very complex inorganic crystals or polymers may be investigated using this approach. In contradiction to the empirical methods, the first-principles approach has more predictive power and further systematic improvements are possible. Of great excitement is the possibility of applying the present method to systems involving surfaces, interfaces, superlattices, and microstructures. Such studies will definitely facilitate the proper materials design and applications in a variety of electro-optical technologies.

## ACKNOWLEDGMENTS

This work was supported by the Office of Naval Research through Grant No. N00014-91-J-1110. One of us (W.Y.C.) would like to thank Professor John Sipe, Dr. D. Moss, Dr. Ed. Ghahramani, Dr. D. C. Allan, and Dr. Z. H. Levine for valuable discussions.

- 
- <sup>1</sup>*Nonlinear-Optical Properties of Materials*, edited by C. M. Bowden and J. W. Hans, Special Issue, J. Opt. Soc. Am. B **6** (1989).
- <sup>2</sup>*Nonlinear Optical Properties of Organic Molecules and Crystals*, edited by D. S. Chemla and J. Zyss (Academic, New York, 1987), Vol. 1.
- <sup>3</sup>*Optical Nonlinearities and Instabilities in Semiconductors*, edited by Hartmut Haug (Academic, New York, 1988).
- <sup>4</sup>S. Schmitt-Rink, D. S. Chemla, and D. A. B. Miller, Adv. Phys. **38**, 89 (1989); A. Miller, D. A. B. Miller, and S. D. Smith, *ibid.* **30**, 697 (1981).
- <sup>5</sup>D. F. Eaton, Science **253**, 281 (1991).
- <sup>6</sup>N. Blombergen, *Nonlinear Optics* (Benjamin, New York, 1965).
- <sup>7</sup>Y. R. Shen, *The Principles of Nonlinear Optics* (Wiley-Interscience, New York, 1984).
- <sup>8</sup>S. Singh, in *Handbook of Laser Science and Technology*, edited by M. J. Weber (CRC, Cleveland, 1986), Vol. III, pt. 1, p. 88.
- <sup>9</sup>P. N. Butcher and D. Cotter, *The Elements of Nonlinear Optics* (Cambridge University Press, New York, 1990).
- <sup>10</sup>See, for example, R. W. Boyd, *Nonlinear Optics* (Academic, New York, 1992).
- <sup>11</sup>J. A. Van Vechten, Phys. Rev. **182**, 891 (1968); B. F. Levine, Phys. Rev. Lett. **22**, 787 (1969).
- <sup>12</sup>J. C. Phillips and J. A. Van Vechten, Phys. Rev. **183**, 709 (1969).
- <sup>13</sup>C. Flytzanis and J. Ducuing, Phys. Rev. **178**, 1218 (1969).
- <sup>14</sup>D. A. Kleinman, Phys. Rev. B **2**, 3139 (1970).
- <sup>15</sup>C. L. Tang and C. Flytzanis, Phys. Rev. B **4**, 2520 (1971).
- <sup>16</sup>M. I. Bell, Phys. Rev. B **6**, 516 (1972).
- <sup>17</sup>C. L. Tang, IEEE J. Quantum Electron. **QE-9**, 755 (1973).
- <sup>18</sup>D. E. Aspnes, Phys. Rev. B **6**, 4648 (1972).
- <sup>19</sup>B. F. Levine, Phys. Rev. B **7**, 2600 (1973).
- <sup>20</sup>M. M. Choy, S. Ciraci, and R. L. Byer, IEEE J. Quantum Electron. **QE-11**, 40 (1975).
- <sup>21</sup>C. Y. Fong and Y. R. Shen, Phys. Rev. B **12**, 2325 (1975).
- <sup>22</sup>D. J. Moss, J. E. Sipe, and H. M. van Driel, Phys. Rev. B **36**, 9708 (1987).
- <sup>23</sup>M. E. Lines, Phys. Rev. B **41**, 3372 (1990); **41**, 3383 (1990); **43**, 11 978 (1991).
- <sup>24</sup>D. J. Moss, E. Ghahramani, J. E. Sipe, and H. M. van Driel, Phys. Rev. B **34**, 8758 (1986).
- <sup>25</sup>M.-Z. Huang and W. Y. Ching, J. Phys. Chem. Solids **46**, 977 (1985).
- <sup>26</sup>M.-Z. Huang and W. Y. Ching, preceding paper, Phys. Rev. B **47**, 9449 (1993).
- <sup>27</sup>E. Ghahramani, D. J. Moss, and J. E. Sipe, Phys. Rev. B **43**, 9700 (1991); **43**, 8990 (1991).
- <sup>28</sup>D. J. Moss, E. Ghahramani, J. E. Sipe, and H. M. van Driel, Phys. Rev. B **41**, 1542 (1990).
- <sup>29</sup>E. Ghahramani, D. J. Moss, and J. E. Sipe, Phys. Rev. Lett. **64**, 2815 (1990); Phys. Rev. B **43**, 8990 (1991).
- <sup>30</sup>E. Ghahramani, D. J. Moss, and J. E. Sipe, Phys. Rev. B **43**, 9269 (1991).
- <sup>31</sup>Z. H. Levine, Phys. Rev. B **42**, 3567 (1990).
- <sup>32</sup>Z. H. Levine and D. C. Allan, Phys. Rev. Lett. **66**, 41 (1991).
- <sup>33</sup>Z. H. Levine and D. C. Allan, Phys. Rev. B **44**, 12 718 (1991).
- <sup>34</sup>Hong-Ru Ma, S. T. Chui, R. V. Kasowski, and W. Y. Hsu, Opt. Commun. **85**, 437 (1991).

- <sup>35</sup>W. Y. Ching, *J. Am. Ceram. Soc.* **71**, 3135 (1990), and references cited therein.
- <sup>36</sup>M.-Z. Huang and W. Y. Ching, *Phys. Rev. B* **45**, 8738 (1992).
- <sup>37</sup>W. Y. Ching and M.-Z. Huang, following paper, *Phys. Rev. B* **47**, 9479 (1993).
- <sup>38</sup>R. C. Miller, *Appl. Phys. Lett.* **5**, 17 (1964).
- <sup>39</sup>See, for example, R. Loudon, *The Quantum Theory of Light* (Clarendon, Oxford, 1983).
- <sup>40</sup>J. A. Armstrong, N. Bloembergen, J. Ducuing, and P. S. Pershan, *Phys. Rev.* **127**, 1918 (1962).
- <sup>41</sup>R. Loudon, *Proc. Phys. Soc. London* **80**, 952 (1962).
- <sup>42</sup>P. N. Butcher and T. P. McLean, *Proc. Phys. Soc. London* **81**, 219 (1963); **83**, 579 (1964); H. Chen and P. B. Miller, *Phys. Rev.* **143**, A683 (1964).
- <sup>43</sup>P. L. Kelley, *J. Phys. Chem. Solids* **24**, 607 (1963); **24**, 1113 (1963).
- <sup>44</sup>B. J. Orr and J. F. Ward, *Mol. Phys.* **20**, 513 (1971).
- <sup>45</sup>E. I. Blount, in *Solid State Physics*, edited by F. Seitz and D. Turnbull (Academic, New York, 1962), Vol. 3, p. 305.
- <sup>46</sup>G. Lehman and M. Taut, *Phys. Status Solidi B* **119**, 9 (1983).
- <sup>47</sup>M. S. Hybertsen and S. G. Louie, *Phys. Rev. B* **34**, 5390 (1986); **37**, 2733 (1988).
- <sup>48</sup>R. W. Godby, M. Schlüter, and L. J. Sham, *Phys. Rev. B* **36**, 6497 (1987).
- <sup>49</sup>M. P. Surh, S. G. Louie, and M. L. Cohen, *Phys. Rev. B* **43**, 9126 (1991).
- <sup>50</sup>R. G. Verbrich, in *Optical Nonlinearities and Instabilities in Semiconductors* (Ref. 3), p. 121; W. Schäfer, *ibid.* p. 133.
- <sup>51</sup>R. A. Soref and H. W. Moos, *J. Appl. Phys.* **35**, 2152 (1964).
- <sup>52</sup>C. K. N. Patel, *Phys. Rev. Lett.* **16**, 613 (1966).
- <sup>53</sup>J. J. Wynne and N. Bloembergen, *Phys. Rev.* **188**, 1211 (1969).
- <sup>54</sup>J. H. McFee, G. D. Boyd, and P. H. Schimidt, *Appl. Phys. Lett.* **17**, 57 (1970).
- <sup>55</sup>J. J. Wynne, *Phys. Rev. Lett.* **27**, 17 (1971).
- <sup>56</sup>B. F. Levine and C. G. Bethea, *Appl. Phys. Lett.* **20**, 272 (1972).
- <sup>57</sup>G. H. Sherman and P. D. Coleman, *J. Appl. Phys.* **44**, 238 (1973).
- <sup>58</sup>M. M. Choy and R. L. Byer, *Phys. Rev. B* **14**, 1693 (1976).
- <sup>59</sup>G. H. Sherman and P. D. Coleman, *J. Appl. Phys.* **35**, 2152 (1964).
- <sup>60</sup>F. G. Parsons and R. K. Chang, *Opt. Commun.* **3**, 173 (1971).
- <sup>61</sup>D. Bethune, A. J. Schmidt, and Y. R. Shen, *Phys. Rev. B* **11**, 3867 (1975).
- <sup>62</sup>H. Lotem, G. Koren, and Y. Yacoby, *Phys. Rev. B* **9**, 3532 (1974).
- <sup>63</sup>R. K. Chang, J. Ducuing, and N. Bloembergen, *Phys. Rev. Lett.* **15**, 415 (1965).
- <sup>64</sup>F. G. Parson and R. K. Chang, *Opt. Commun.* **3**, 173 (1971).